

tations [6]. These measurements caused a resurgence of interest in nucleon structure, and shed light on the importance of quark orbital angular momentum. More recent double-polarization experiments measured the neutron electric form factor  $G_E^n$  up to a  $Q^2$  of 3.4 GeV $^2$  (E02-013) [7], and showed behavior that was generally consistent

with the earlier proton results. The neutron results, when combined with the proton results, made it possible to extract the form factors for the individual up- and down-quark flavors [8]. Significantly different  $Q^2$  dependence was found between the two quarks, a difference that some theorists have interpreted as evidence for the importance of thermal correlations.

The multiple surprises that have emerged from the study of nucleon elastic form factors have been well documented [9]. Nuclear-polarized noble gases have been proven to be very useful in various applications, such as polarized targets for electron scattering experiments [1], magnetic resonance imaging [2] and neutron scattering experiments [3]. Polarized  ${}^3\text{He}$  has been particularly useful for studying spin-dependent interactions involving neutrons because, to first-order approximation, a  ${}^3\text{He}$  nucleus has a pair of protons with paired spins and a single neutron that carries most of the nuclear spin. Free neutrons are not used as targets because they decay with a lifetime of about 14 minutes, 42 seconds.

## 1.1 Motivation and Approved JLab Experiments

The neutron electromagnetic form factors,  $G_E^n$  and  $G_M^n$  play essential roles for understanding nucleon structure. At non-relativistic energies, they are the Fourier transforms of the electric charge and magnetic moment distributions. Even at relativistic energies, the elastic form factors provide unique information on the transverse structure of the nucleon [4, 5]. Double-polarization experiments on the proton showed that the ratio  $G_E^p/G_M^p$ , declines <sup>nearly</sup> linearly as  $Q^2$  increases, in sharp contrast to expec-

of the proton's electric  
and magnetic elastic  
form factors,

the four momentum  
transfer squared

tations [6]. These measurements caused a resurgence of interest in nucleon structure, and shed light on the importance of quark orbital angular momentum. More recent double-polarization experiments measured the neutron electric form factor  $G_E^n$  up to a  $Q^2$  of  $3.4 \text{ GeV}^2$  (E02-013) [7], and showed behavior that was generally consistent with models that described well the earlier proton results. The neutron results, when combined with the proton results,<sup>also</sup> made it possible to extract the form factors for the individual up- and down-quark flavors [8]. Significantly different  $Q^2$  dependence was seen for the up- and down-quarks, a difference that some theorists have interpreted as evidence for the importance of diquark correlations.

The multiple surprises that have emerged from the study of nucleon elastic form factors at Jefferson Laboratory have underscored the value of performing such studies at high values of  $Q^2$ . For the neutron, predictions for the behavior of the ratio of the electric and magnetic elastic form factors,  $G_E^n/G_M^n$ , vary significantly from one model or calculation to another. A particularly compelling example, based on the Dyson-Schwinger Equation (DSE) formalism, predicts a dramatic turnover and zero crossing in the vicinity of  $Q^2 = 10 \text{ GeV}^2$  [9]. The verification of this prediction would have profound impact on our understanding of nucleon structure. An important part of the future program at JLab to explore the high- $Q^2$  behavior of the elastic nucleon form factors is the Super Bigbite Spectrometer (SBS) program. The SBS experiment to measure  $G_E^n/G_M^n$  up to  $Q^2 = 10 \text{ GeV}^2$ , E12-09-016, is a major motivating factor for the work described in this thesis. The count rate associated with the elastic form factors drops off very quickly with increasing  $Q^2$ . This in turn puts pressure on all aspects of the experiment to achieve adequate statistics, including running the polarized  ${}^3\text{He}$  target at high luminosity.

Another important issue in understanding nucleon structure is the spin structure associated with the quarks. Polarized deep inelastic scattering provides a window

*into*

the spin carried by the quarks, and a particularly useful observable is the spin asymmetry  $A_1^n$ , ~~that~~ <sup>describing</sup> that describes the spin dependence of the virtual photo absorption cross section. It is particularly useful to measure  $A_1^n$  at high values of Bjorken  $x$ , where several predictions exist. Both constituent quark models and perturbative QCD predict that  $A_1^n \rightarrow 1$  as  $x_{Bj} \rightarrow 1$ , but it is also the case that count rates drop quickly toward high values of  $x_{Bj}$ . Two experiments are currently approved at JLab that will measure  $A_1^n$  up values of  $x_{Bj}$  in excess of 0.7; they are E12-06-122 in Hall A, and E12-06-110 in Hall C. Both of these experiments will require a polarized  ${}^3\text{He}$  target capable of running at high luminosity and thus depend critically on the work described here.

## 1.2 Overview of Recent Target Development

An early use of polarized  ${}^3\text{He}$  targets in electron scattering experiments was at the Stanford Linear Accelerator Center (SLAC) in the year of 1992. The experiment was known as E142 and investigated the spin structure of neutrons [1]. Recent experiments were conducted at Jefferson Laboratory (JLAB) in Newport News, Virginia, such as the aforementioned E02-013, also known as “Measurement of the Neutron Electric Form Factor  $G_E^n$  at High  $Q^2$ ”. Experiments that investigated single spin asymmetries [10] also included E06-10, E06-014 and E05-015.

*Replace with \**

The  ${}^3\text{He}$  targets used in these experiments were polarized with the technique of Spin-Exchange Optical Pumping (SEOP). Fig. 1.1 shows schematically a typical target, also referred to as a “target cell”. These cells were made of GE180 glass and used a two-chambered design. The top chamber, known as the pumping chamber, is where  ${}^3\text{He}$  is polarized through SEOP. The bottom chamber, known as the target chamber, is where electron scattering occurs. The two ends of the target chamber

*gluotation  
marks*

[Other experiments involved the investigation of single-spin asymmetries in semi-inclusive deep inelastic scattering.  
[Qian et al., attached to email]]

where electron beam enters and exits are known as the “end windows”. Great effort has been made in our lab to develop this generation of cells. Alkali-hybrid SEOP together with narrowband laser-diode arrays have increased the  $^3\text{He}$  polarization from 37% to 70%. Among other things, we also carefully studied an additional spin relaxation mechanism that limits the maximum achievable  $^3\text{He}$  polarization, which is referred to as the “X Factor”. Analysis of data accumulated through developing this generation of target cells were thoroughly discussed in Ref. [11], part of which will be presented in chapter 4.

can be  
characterized  
by something

that comes with higher beam current is that the glass windows of traditional design are not likely to survive the experiments. Our group started exploring the option of using metal end windows years ago. One of such a target cell the first problem to solve is how to incorporate metal without introducing spin relaxation and still using pressure gas. This is a brand new technique that may have a profound impact on future experiments. Although no metal end windows have been fully developed. After all no metal end windows have been fully examined multiple glass cells with different kinds metal tubes (much larger in area) and windows that will be used in JLAB experiments attached, we have developed a reliable way of incorporating metal end windows without introducing spin relaxation issues. We believe that in our test cells, the metal tubes were connected to Pyrex glass with high pressure (13) and stayed intact through high pressure tests. After exploring

**Figure 1.1:** A schematic representation of a target cell. The dimensions of different parts of the cell are not to scale.

### 1.3 New Generation Target Cells

The future experiments planned for the 12GeV era after the upgrade will be much more demanding in terms of target cell performance. In particular, there is a desire

to run experiments with higher luminosity, where luminosity is the product of gas density in the target, interaction length and beam current. Increased luminosity will lead to more interactions that depolarize the target. We have designed and tested a new style cell that utilizes convection instead of diffusion to increase the rate at which the polarization in the target chamber is replenished by polarized gas from pumping chamber [12]. We have obtained over 50% polarization with controllable convection speed so far.

An additional problem that comes with higher beam current is that the glass end windows of traditional design are not likely to survive the experiments. Our group started exploring the option of using metal end windows since eight years ago. Fig 1.2 shows an example configuration of such a target. The first problem to solve is to find out the correct material and the proper technique to incorporate metal without introducing significant spin relaxation while still being able to hold high pressure gas (12 atm) inside. This is a brand new technique that may have a profound impact on future cell designs once fully developed. Although no metal end windows have been tested so far, through carefully examining multiple glass cells with different kinds metal tubes (much larger in area compared to the end windows that will be used in JLAB experiments) attached, we have developed a reliable way of incorporating metal into target cells without introducing excessive spin relaxation rates. We believe the next generation target cells used in the 12GeV era will be able to utilize metal end windows. In our test cells, the metals tubes were connected to Pyrex glass with Houskeeper seals [13] and stayed intact through high pressure tests. After exploring options such as pure copper, gold coated copper, titanium, stainless steel, gold coated titanium, we have established that electroplating gold on a copper substrate yields the best result so far. We have achieved a 15.6 h relaxation time with a Pyrex cell that had a 5" long by 1" diameter gold coated copper tube attached horizontally. The additional

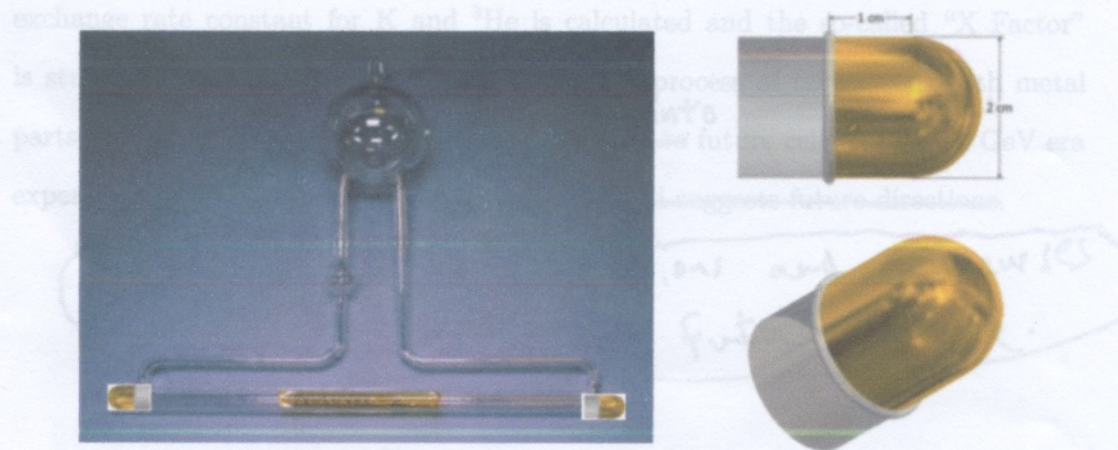


**Figure 1.2:** A diagram of convection style target cell with metal end windows.

relaxation rate introduced by the metal surface is proportional to the area of the gold ~~glass-and-metal~~ surface. By comparing relaxation rates of test ~~metal~~ cells with pure-glass control ~~extracted~~, the relaxation rate due to the gold surface was ~~extrapolated~~. With this result, we believe the ~~relaxation~~ rate introduced by small metal windows in a target will be less than  $1/130.6 \text{ hr}^{-1}$ . To the best of our knowledge, our group was the first to have proved the potential of incorporating metal ~~into~~ target cells in the presence of alkali vapor.

## 1.4 Structure of This Thesis

This thesis focuses on both ~~a~~ discussion ~~of~~ the development of high-performance polarized  $^3\text{He}$  targets that utilize spin-exchange optical pumping (SEOP) and the development of future target cells that incorporate metal end windows. Chapter 2 gives a general description of SEOP. Chapter 3 introduces polarimetry techniques used in our lab for target cell characterization. Chapter 4 discusses the results ~~collected in over a decade of~~ <sup>s</sup> collected in our lab from ~~the over a decade~~ development of  $^3\text{He}$  target cells, in which the spin-

exchange rate constant for K and  $^3\text{He}$  is calculated and the so-called "X Factor" is studied. Chapter 5 presents the development process of target cells with metal parts that aims to incorporate metal end windows  $\xrightarrow{\text{into}}$  future cells for the  $^{12}\text{GeV}$  era experiments. Chapter 6 ~~summarizes this thesis and suggests future directions.~~

*presents some conclusions and discusses  
the implications for future work.*

## Introduction

$$(F.S.)^n \pi^+ H = A$$

Polarized noble gases have been proposed for various applications, such as polarized targets for electron scattering experiments [1], magnetic resonance imaging [2] and neutron scattering experiments [3]. Polarized  $^3\text{He}$  has been particularly studied for spin-dependent interactions involving nucleons because, to first-order approximation, a  $^3\text{He}$  nucleus has a pair of protons with paired spins and a single neutron that carries most of the nuclear spin. Free neutrons are not used as targets because they decay with a lifetime of about  $10^{-27}$  seconds.

### 1.1 Motivation and Approach to the Experiments

The nuclear electromagnetic form factors  $G_E^N$  and  $G_M^N$  play essential roles for understanding nuclear structure. At non-relativistic energies, they are the Fourier transforms of the electric charge and magnetic moment distributions. Even at relativistic energies, the elastic form factors provide unique information on the internal structure of the nucleus [4, 5]. Double-polarization experiments on the proton showed that  $G_E^p \propto Q^2$  and  $G_M^p \propto Q^2$ , an  $Q^2$  increase, in sharp contrast to ex-

$\xrightarrow{\text{MS}} G_E^N \propto Q^2$  in the magnetic black box  
with hadrons,

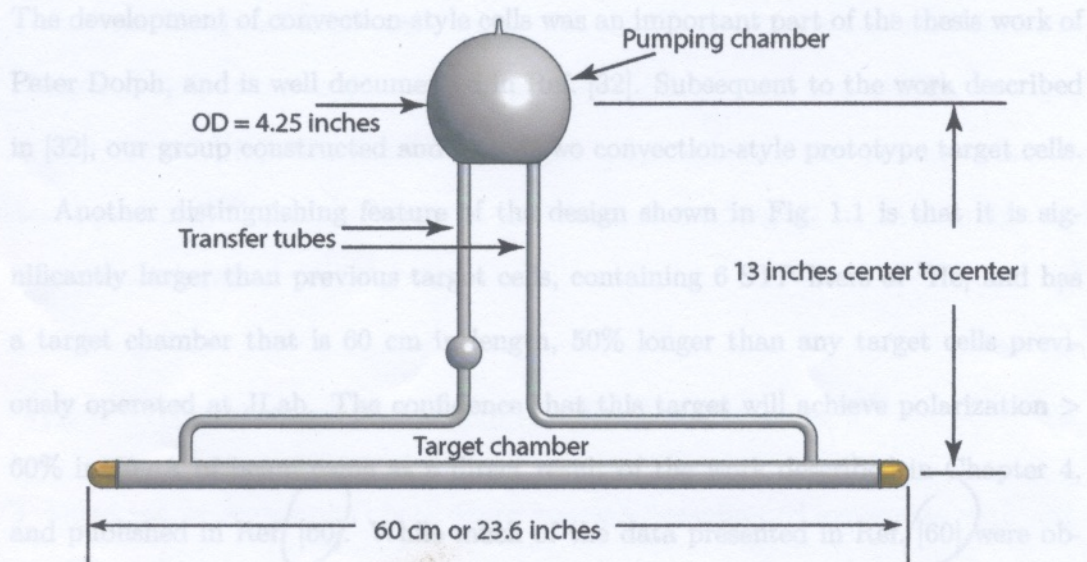
$\xrightarrow{\text{MS}} p^2 \cdot S$

the four momentum transfer & gluon

# Chapter 1

## Conclusions and Discussion

The work presented in this thesis has made it possible to design and begin producing the next-generation polarized  $^3\text{He}$  targets for use at Jefferson Laboratory. These next-generation targets are being developed and produced in two steps, which are referred to internally at JLab as the Stage-I and Stage-II designs. The Stage-I targets contain a volume of 3 STP liters of  $^3\text{He}$ , the same quantity that was contained in the cell Antoinette, the results from which were described in Chapter 4. The Stage-II targets, while similar in geometry, are larger and will contain 6 STP liters of  $^3\text{He}$ . At the time of this writing, the first Stage-I target cell has already been produced and is undergoing bench tests. When using only half the design laser power, the target has already achieved a polarization of 65%, higher than what is needed for actual running (although we note that this is without the depolarizing effects of an electron beam). These early tests are quite encouraging when extrapolated to the full laser power that will be used. Also, the conceptual design of the Stage-II target cells has been completed, and was evaluated in a review, conducted in March of 2016, of the



The development of convection-style cells was an important part of the thesis work of Peter Dolph, and is well documented [31]. Subsequent to the work described in [32], our group redesigned and built a convection-style prototype target cell.

Another important difference with the design shown in Fig. 1.1 is that it is significantly larger than previous target cells, containing a target chamber that is 60 cm long, 50% longer than any target cells previously operated at Hall A. The longer available length will achieve polarization > 60% in a reasonable time period.

**Figure 1.1:** Design of next-generation target for upcoming SBS  $G_E^n$  experiments.

polarized  $^3\text{He}$  target that is being built for the Hall A Super Bigbite Spectrometer (SBS) experiment to measure  $G_E^n$ , the electric form factor of the neutron. The design for the SBS  $G_E^n$  target is shown in Fig 1.1.

## 1.1 Overall Design of Next-Generation Polarized $^3\text{He}$ Targets

The target-cell design illustrated in Fig. 1.1 incorporates multiple features that distinguish it from earlier polarized  $^3\text{He}$  targets based on spin-exchange optical pumping. The basic geometry is what we refer to as a “convection-style” cell, in which the pumping and target chambers are connected by two transfer tubes, one of which is heated, resulting in controllable convective flow between the target’s two principle chambers.

The development of convection-style cells was an important part of the thesis work of Peter Dolph, and is well documented in Ref. [32]. Subsequent to the work described in [32], our group constructed and tested two convection-style prototype target cells.

Another distinguishing feature of the design shown in Fig. 1.1 is that it is significantly larger than previous target cells, containing 6 STP liters of  $^3\text{He}$ , and has a target chamber that is 60 cm in length, 50% longer than any target cells previously operated at JLab. The confidence that this target will achieve polarization  $> 60\%$  in  $60 \mu\text{A}$  of beam came as a direct result of the work described in Chapter 4, and published in Ref. [60]. While much of the data presented in Ref. [60] were obtained prior to the work described here, most of the analysis was performed as part of this work, including a determination of the coefficient characterizing spin-exchange between potassium and  $^3\text{He}$ .

Data included in ref. [60] that were specifically obtained as part of this thesis work included all of the studies of the cell Antoinette, which contained roughly 3 STP liters of  $^3\text{He}$ . While target-cells containing 3 STP liters of  $^3\text{He}$  were used during the first Hall A  $G_E^n$  experiment, commercial narrow-band high-power diode-laser arrays, which are critical to achieving high performance, were not yet available during both testing and the experiment itself. Thus, Antoinette was the first target cell tested with narrow-band lasers that contained both 3 STP liters of  $^3\text{He}$  and an alkali-hybrid mixture for optical pumping. As such, Antoinette became a proof of principle for both of the above-mentioned prototype convection-style target cells, as well as the first of the Stage-I target cells that is undergoing testing at the time of this writing.

In short, the work presented here provided the basis for designing the high-performance Stage-I and Stage-II target cells that will be used in future JLab ex-

The relaxivity for Pyrol can be computed to be  $0.034 \text{ cm}^2/\text{mOe}$ , and when compared with Gold Bush, indicates a relaxivity of  $0.13 \text{ cm}^2/\text{m}$  for the metal.

periments. The proof-of-principle began with the cell Antoinette, and continued with the two prototype convection-style target cells (both of which also contained roughly 3 STP liters of  ${}^3\text{He}$ ). The first actual Stage-I target cell looks very promising in early tests, providing further confidence in the design of the Stage-II target cells that will soon be produced.

During the 6 GeV era where only  $10\text{-}15 \mu\text{A}$  was used, glass end windows were

## 1.2 Incorporating Metal End Windows

Prior to the work described here, there was only very limited experience with spin-polarized noble gases in cells containing metal. The reason is that the introduction of any new material generally causes spin relaxation greatly in excess to that caused by the walls of the glass container. The target-cell design shown in Fig. 1.1, however, incorporates metal end windows so that even a fairly intense electron beam will not cause the target cell to rupture, even after multiple weeks of operation. One of the important achievements of the current work was the development of a technique for producing metal surfaces that induce spin relaxation at an acceptably slow rate. We further have demonstrated a means for making transitions between glass and metal, even when operating at the high pressures used in our polarized  ${}^3\text{He}$  targets. We describe next why metal end windows based on the techniques demonstrated here are likely to have an almost negligible effect on the overall performance of our target cells.

The spin relaxation caused by metal end windows in future target cells can be calculated using the equation  $\Gamma_{\text{metal}} = \rho_{\text{metal}} S_{\text{metal}} / V_{\text{total}}$  (see Chapter 2.4). Furthermore, the relaxivity associated with metal can be extracted by comparing a ~~glass-metal-glass~~ ~~glass - and - metal~~

The relaxivity for Pyrah can be computed to be  $0.0314 \text{ cm/hr}$ , and when compared with GoldRush, indicates a relaxivity of  $0.123 \text{ cm/hr}$  for the metal

test cell (such as GoldRush in Table ??) with an all-glass control cell (such as Pyrah

in Table ??). The resulting relaxivity is  $0.03144 \text{ cm/hr}$  and  $0.1231 \text{ cm/hr}$  for metal.

Using this relaxivity and the designed dimensions for the target end windows, the additional relaxation times would be  $1/130.6 \text{ hr}^{-1}$  for Stage-I cells and  $1/261.2 \text{ hr}^{-1}$  for Stage-II cells.

During the 6 GeV era where only  $10-15 \mu\text{A}$  was used, glass end windows were already running into risk of rupturing after 4-6 weeks of being exposed to ~~the electron beam~~. If it was solely due to radiation damage, one ~~would~~ expect the glass windows to rupture after roughly a week of being used in ~~an~~ electron beam of  $60 \mu\text{A}$ , which ~~would~~ be much less than the time required for far from enough for the experiments to complete. On the other hand, experience at JLab suggests that even very thin metal windows ~~should still~~ be able to survive the electron beams. As an example, aluminum as thin as 2 mils has been routinely used in JLab without failing. The fact that metal end windows will conduct heat better further suggests that they will be more suitable for ~~experiments planned for the 12~~ ~~the planned~~ GeV era.

Copper test pieces with thin hemispherical end caps using OFHC copper and aluminum will be made into test cells based on the design shown in Fig. 1.1 before the planned experiments are conducted.

### 1.3 Summary

We have confidence that convection style targets with metal end windows will not only give high  $^3\text{He}$  polarization in both  $\text{P}$  and  $\text{B}$ , but also survive the high electron beam currents planned for the future experiments. The work done in this thesis has demonstrated that the additional spin-relaxation rate due to surfaces in metal end

while some work remains to determine the optimal configuration for the window itself, the work presented here provides the critical technology that previously prevented us using metal end